

# Derivation and Characterization of an Extra-Axial Chordoma Cell Line (EACH-1) from a Scapular Tumor

By Amalia M. DeComas, MD, Patrice Penfornis, MSc, Michael R. Harris, BSc, Mark S. Meyer, MD, and Radhika R. Pochampally, PhD

*Investigation performed at Ochsner Medical Center, New Orleans, and Tulane University Health Sciences Center, New Orleans, Louisiana*

**Background:** Extra-axial chordomas are rare low-grade malignant tumors thought to arise from notochordal remnants in the extra-axial skeleton. Few studies have been done on this neoplasm because of its rarity. In addition, there is a lack of a good in vitro model on which to perform more characterization.

**Methods:** We describe a twenty-eight-year-old man with a mass in the right scapula. Cytomorphology and immunohistochemistry, including brachyury staining, were used to formulate the final diagnosis. A fragment of the tumor was placed in culture, and cells obtained were injected subcutaneously in an immunocompromised mouse. From the tumor developed in mice, a cell line has been derived and characterized by fluorescence-activated cell-sorting analysis, karyotyping, clonogenicity, and cell and tumor growth curves.

**Results:** Cytomorphology on the tumor showed nests of round cells with vacuoles and also physaliferous-like cells with uniform nuclei. Immunohistochemistry revealed a tumor positive for vimentin, moderately positive for S-100 and cytokeratin AE1/AE3, weakly positive for epithelial membrane antigen, and negative for p63 and cytokeratin (CK)-7. Further analysis revealed the tumor was diffusely and strongly positive for brachyury. The cell line derived from the tumor showed rapid doubling-time, a strong expression of mesenchymal cell surface markers, a karyotype of diploid or hypotetraploid clones with numerous chromosomal aberrations, and the ability to form colonies without attachment and to form tumors in immunocompromised mice.

**Conclusions:** The diagnosis of the extra-axial chordoma is difficult but can be resolved by the detection of a strong brachyury expression. In addition, the derivation of a human extra-axial chordoma cell line could be a useful tool for the basic research of this rare neoplasm.

**Clinical Relevance:** We describe the importance of brachyury staining in the diagnosis of this tumor. The extra-axial chordoma cell line (EACH-1) may also provide a new research tool to establish new ways of diagnosing and treating this rare malignancy.

A chordoma is a rare low-grade malignant tumor thought to arise from vestigial notochordal tissue. The classic site is in the axial skeleton. Studies vary on the prevalence of the sites; however, approximately one-half are located in the sacrococcygeal region, with the others distributed mainly to the remainder of the spine and the sphenoccipital region<sup>1,2</sup>.

The tumor is histologically composed of variably sized myxoid lobules, with multivacuolated, large epithelioid or so-called physaliferous cells<sup>3</sup>. When a tumor with histologically

similar features is encountered in the extra-axial skeleton, then the differential diagnosis broadens to include other neoplasms such as parachordoma, malignant myoepithelioma, extra-skeletal myxoid chondrosarcoma, and extra-axial chordoma. The staining patterns and cytogenetic characteristics are variable, so arriving at an accurate diagnosis can be challenging<sup>4-6</sup>. Brachyury is thought to be a specific marker for notochord-derived tumors, and a positive stain on a peripheral musculoskeletal tumor provides strong support for the diagnosis of an extra-axial chordoma<sup>7,8</sup>. Wide excision is the treatment of

**Disclosure:** In support of their research for or preparation of this work, one or more of the authors received, in any one year, outside funding or grants in excess of \$10,000 from the Louisiana Cancer Research Consortium; HCA—The Healthcare Company; and the Louisiana Gene Therapy Research Consortium. Neither they nor a member of their immediate families received payments or other benefits or a commitment or agreement to provide such benefits from a commercial entity.

choice of all chordomas. They have a high risk of local recurrence, and they also metastasize<sup>9,10</sup>.

The lack of a good in vitro model on which to perform more extensive characterization of this tumor led us to explore the possibility of obtaining a sustainable cell line to aid with further research. We present these data to describe the case of a patient with an extra-axial chordoma, emphasizing the diagnostic challenges with the hope that the development of our cell line will help to further evaluate this tumor in future studies. The patient was informed that data concerning the case would be submitted for publication, and he consented.

## Materials and Methods

### Case Report

A twenty-eight-year-old man presented for evaluation of a mass in the right shoulder. He had a one-year history of pain in the right shoulder, both at rest and with activity, with no history of trauma. There was no other relevant clinical history. Plain radiographs showed a subtle destructive pattern within the scapular body (Fig. 1-A). The magnetic resonance imaging showed a partially enhancing solid mass within the belly of the right supraspinatus muscle. It was oval shaped and well circumscribed. The mass measured  $6.6 \times 4.7 \times 3.4$  cm (Fig. 1-B), exhibited markedly high intensity on the short tau inversion recovery (STIR) sequence, and was relatively isointense to muscle on the T1-weighted sequences. There was destruction of the posterior scapular spine, suggesting invasion of the adjacent cortex. Computed tomography scans of the chest, abdomen, and pelvis showed no abnormalities.

An initial computed tomography-guided needle biopsy was performed because of the concern of malignancy and the difficulty in accessing the mass. It revealed nests of small round cells, many with vacuoles. The cells had uniform, oval-shaped nuclei containing small amounts of eosinophilic cytoplasm (Fig. 2-A). The tumor was strongly positive for vimentin, fo-

cally positive for S-100, moderately positive for cytokeratin AE1/AE3 (Figs. 2-B, 2-C, and 2-D), and negative for p63. A preliminary diagnosis was a parachordoma, or malignant myoepithelioma of the soft tissues.

A wide resection of the tumor was then performed through a posterior approach. Care was taken to excise a cuff of normal tissue surrounding the mass in order to prevent local recurrence. It was also necessary to osteotomize a portion of the scapula to remove the reactive bone. Histological examination revealed clear margins. The resected tumor consisted of a cellular neoplasm composed of physaliferous-like cells with uniform nuclei. It was multinodular and composed of cords of large, partially vacuolated, epithelioid cells in a myxoid matrix (Figs. 2-E and 2-F). Further immunohistochemistry stains were identical to the frozen section with the addition of a weakly positive epithelial membrane antigen (Fig. 3-A) and a negative CK-7. A brachyury antibody stain (polyclonal brachyury antibody, diluted at a ratio of 1:50; Santa Cruz Biotechnology, Santa Cruz, California) was diffusely and strongly positive (Fig. 3-B). This confirmed the diagnosis of an extra-axial chordoma. The patient was doing well clinically with no recurrence or metastasis at two years of follow-up.

The tumor sample was mechanically dissociated with a scalpel into 1-mm pieces and plated in 20 mL of Dulbecco modified Eagle medium (DMEM; Gibco Invitrogen, Grand Island, New York) with 10% fetal bovine serum (Atlanta Biologicals, Lawrenceville, Georgia) and 1% penicillin-streptomycin (Gibco Invitrogen). The media was changed every two to three days. After ten days, some adherent cells grew from the tumor pieces in a monolayer. Once cells reached 70% to 80% confluency, they were lifted with use of 0.25% trypsin-EDTA (Gibco Invitrogen) and analyzed by flow cytometry. The high expression of cell surface markers CD73a, CD105, and CD166, and the lack of expression of CD11b, CD34, CD45, and CD79a (Table I) confirmed their derivation from a mesenchymal lineage<sup>11</sup>.



Fig. 1-A

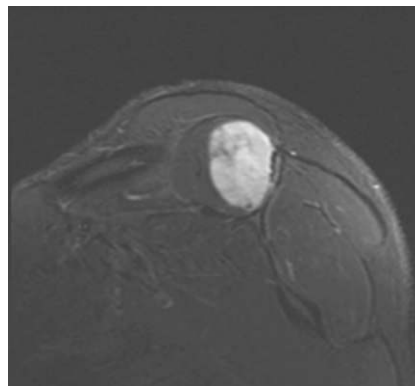


Fig. 1-B

**Fig. 1-A** An anteroposterior radiograph of the right shoulder, showing a subtle destructive pattern within the scapular body. **Fig. 1-B** A coronal slice of a STIR sequence (short T1/Tau Inversion Recovery) magnetic resonance image of the shoulder, showing a partially enhancing solid mass within the belly of the right supraspinatus muscle. It was well circumscribed and measured  $6.6 \times 4.7 \times 3.4$  cm. The mass exhibits markedly high intensity on the STIR sequence.

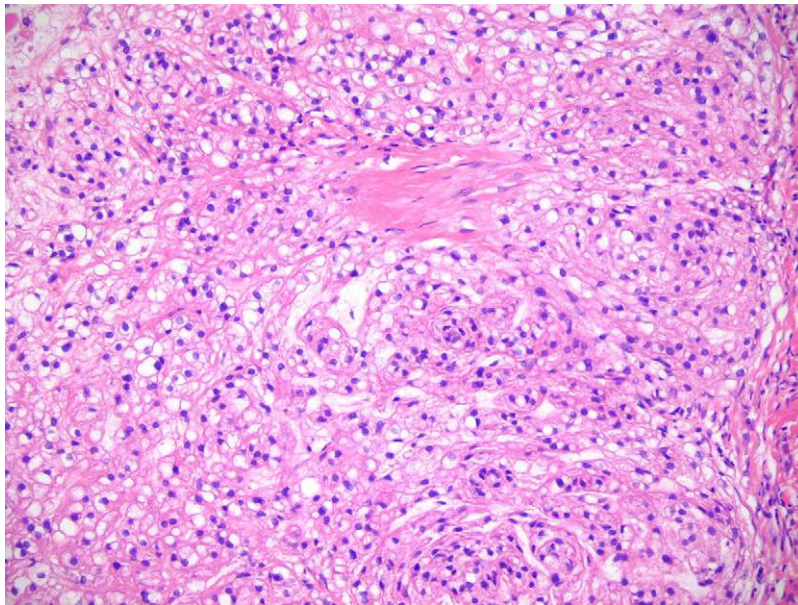


Fig. 2-A

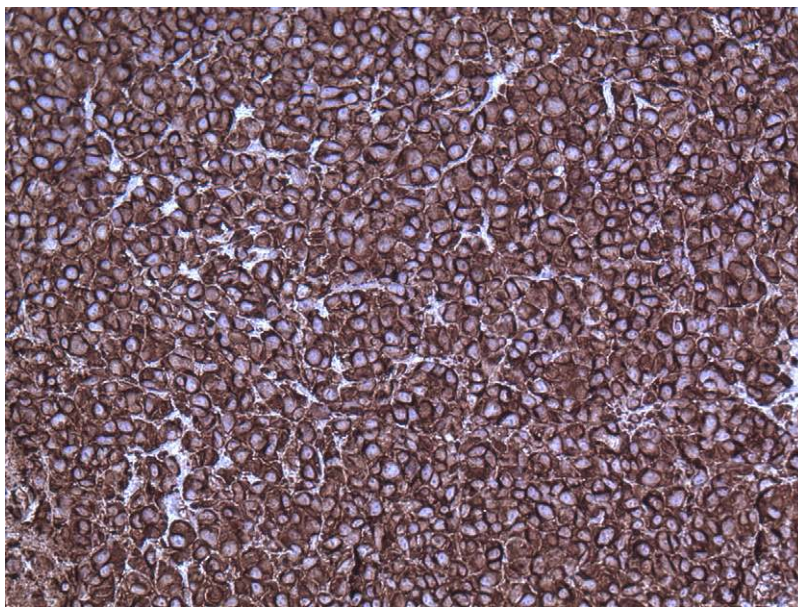


Fig. 2-B

Hematoxylin and eosin staining of a tumor biopsy specimen (Fig. 2-A). Immunostaining for vimentin (Fig. 2-B), S-100 (Fig. 2-C), and cytokeratin AE1/AE3 (Fig. 2-D) ( $\times 10$  for all). Hematoxylin and eosin staining of the resected tumor at  $20\times$  magnification (Fig. 2-E) and at  $80\times$  magnification (Fig. 2-F).

One million cells were injected subcutaneously into the posterior abdominal flank of a nude (*nu/nu*) mouse according to an approved protocol from the Tulane University Institutional Animal Care and Use Committee. After ten weeks, a growing tumor was detected at the site of injection, and it was allowed to grow until it reached 5 mm in diameter. The tumor was removed from the mouse after it was killed twelve weeks after injection, dissected in 1-mm pieces, and placed in culture

medium from which we derived the new extra-axial chordoma cell line named EACH-1 (extra-axial chordoma-1).

#### Flow Cytometry

A volume of  $3 \times 10^5$  cells was concentrated by centrifugation at 500 g for five minutes and suspended in 50  $\mu\text{L}$  of phosphate-buffered saline solution containing 1% (w/v) bovine serum albumin and the fluorescent-labeled antibodies (BD Phar-



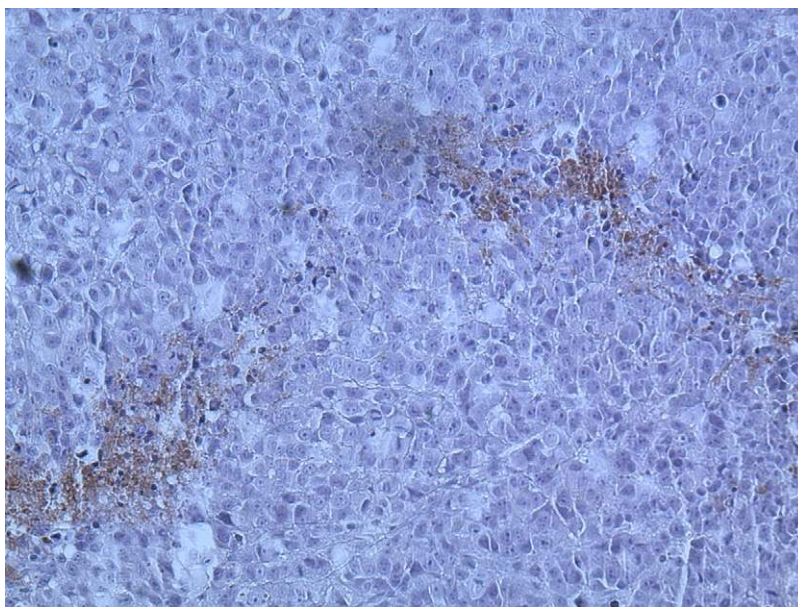


Fig. 2-C

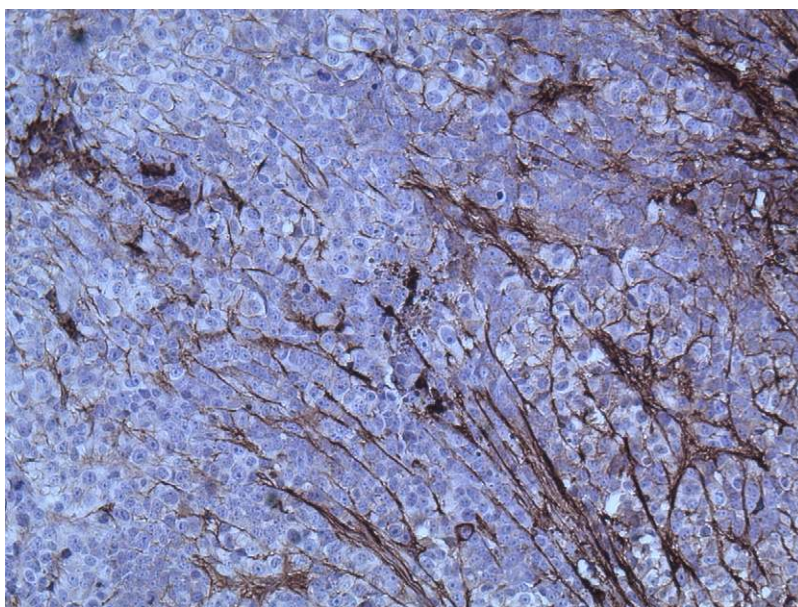


Fig. 2-D

mingen, San Jose, California) indicated in Table I. The samples were incubated for thirty minutes at room temperature and then were washed three times in phosphate-buffered saline solution by centrifugation. The samples were analyzed by a Cytomics FC-500 flow cytometer (Beckman Coulter, Miami, Florida). The percentage of positive cells for each marker was determined by the ratio of positive events compared with the negative control (CXP software; Beckman Coulter).

#### *Growth Curve Assay*

Extra-axial chordoma-derived cells were seeded into two twelve-well plates with 1 mL of DMEM with 10% fetal bovine serum media (500 cells per well). Three wells were trypsinized

each day, and cells were counted for total cell number with use of a hemocytometer for eight days.

#### *Tumor Growth Assay*

Extra-axial chordoma-derived cells were grown to 70% to 80% confluency and then were lifted with trypsin and counted with use of a hemocytometer. A volume of  $10 \times 10^6$  cells was suspended in 200  $\mu$ L of Hanks balanced salt solution (Gibco Invitrogen). Subcutaneous injections of cells into the posterior abdominal flank of six to eight-week-old *nu/nu* mice were carried out in triplicate. Perpendicular tumor diameters were measured biweekly with use of digital calipers, and the volume calculated from the formula:  $4/3 \times$

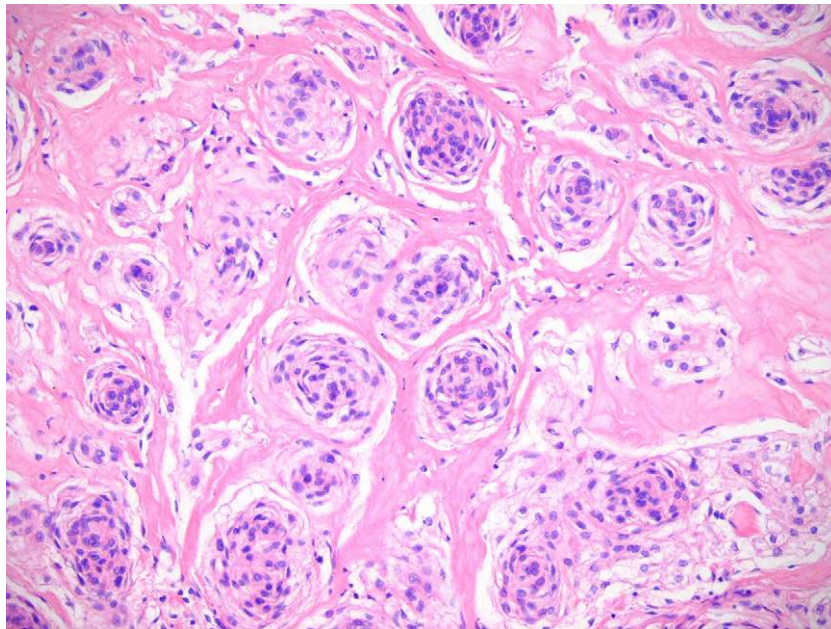


Fig. 2-E

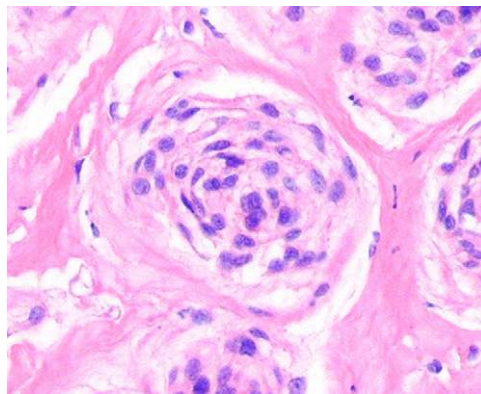


Fig. 2-F

$\pi \times L \times M^2$ , where L is the larger radius and M is the smaller radius.

#### Western Blotting

Cells were prepared and lysed in buffer (RIPA lysis buffer; Santa Cruz Biotechnology) supplemented with protease inhibitor cocktail, and protein concentration was determined (BCA protein assay kit; Pierce Biotechnology, Rockford, Illinois). The cell lysate (20  $\mu$ g of total protein) was fractionated by sodium dodecyl sulfate-polyacrylamide gel electrophoresis (NuPAGE Novex 4-12% Bis-Tris gels; Invitrogen, Carlsbad, California). The sample was transferred to a filter (Immobilon-P PVDF membrane; Millipore, Billerica, Massachusetts) by electroblotting (XCell II Blot Module; Invitrogen). The filter was blocked for two hours with Tris-buffered saline solution (TBS [Sigma, St. Louis, Missouri]; phosphate-buffered saline solution containing 0.05% Tween 20) added with 5% nonfat dry milk and then incubated overnight at 4°C with a rabbit polyclonal brachyury antibody (Bry, clone H-210, number sc-20109; Santa

Cruz Biotechnology) diluted at a ratio of 1:200 in Tris-buffered saline solution with 1% nonfat dry milk. The membrane was washed three times for ten minutes each with Tris-buffered saline solution. Bound primary antibody was detected by incubating for one hour with horseradish peroxidase-conjugated goat anti-rabbit immunoglobulin G (IgG) (Chemicon Millipore, Billerica, Massachusetts). The filter was washed and developed with use of a chemiluminescence assay (Visualizer Spray and Glow ECL detection system; Upstate Biotechnology, Lake Placid, New York).

#### Immunohistochemistry

Slide sections were deparaffinized and rehydrated. Antigen retrieval was performed by using a vegetable steamer containing a boiling solution of sodium citrate buffer (10 mM sodium citrate and 0.05% Tween 20; pH 6.0) for thirty minutes, then slides were washed twice for five minutes in Tris-buffered saline solution with 0.025% Triton X-100. Sections were blocked in 10% normal goat serum with 1% bovine se-



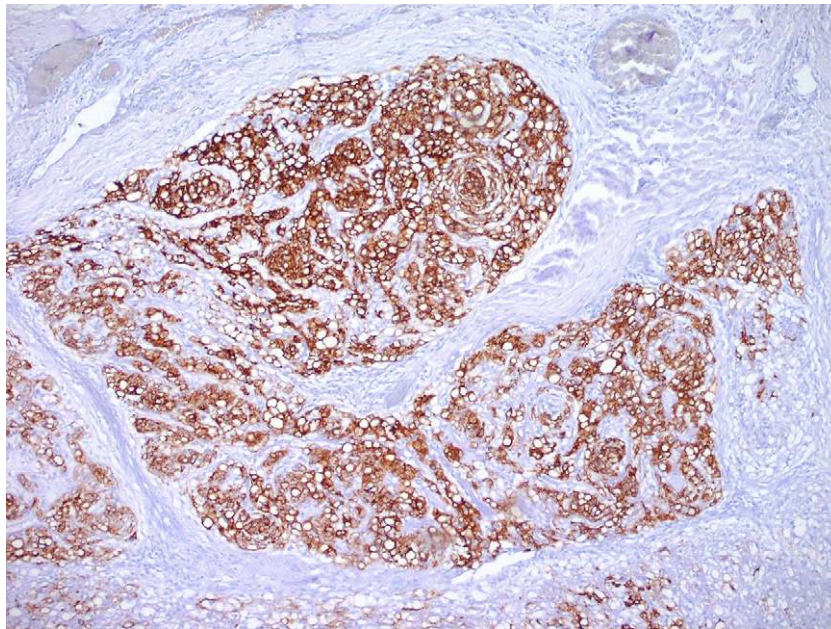


Fig. 3-A

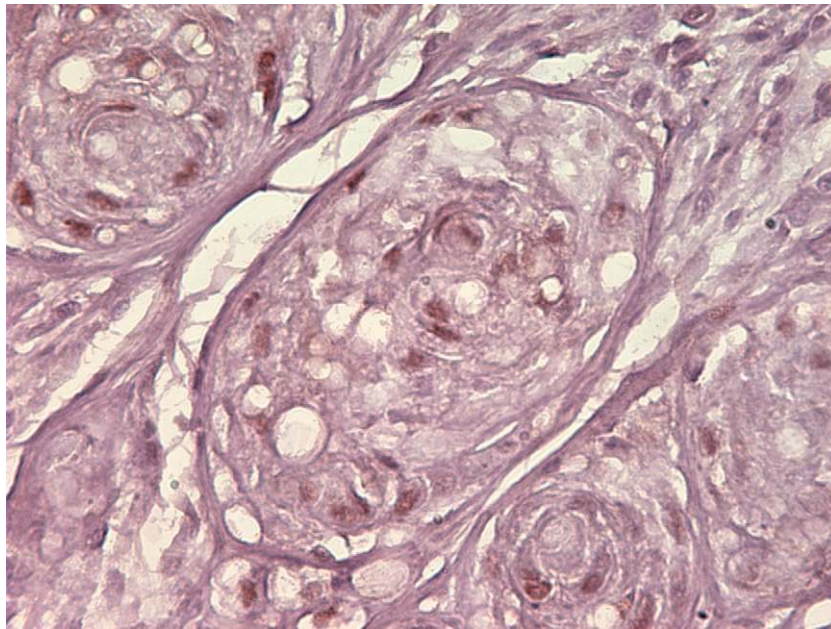


Fig. 3-B

**Fig. 3-A** Epithelial membrane antigen immunostaining ( $\times 20$ ). **Fig. 3-B** Brachyury immunostaining ( $\times 80$ ).

rum albumin in Tris-buffered saline solution overnight at 4°C and incubated for twenty-four hours with a rabbit polyclonal Bry antibody (clone H-210, number sc-20109; Santa Cruz Biotechnology) diluted at a ratio of 1:50 in Tris-buffered saline solution with 1% bovine serum albumin. Negative control slides were obtained by incubating with isotype rabbit IgG. Slides were rinsed twice for five minutes in Tris-buffered saline solution with 0.025% Triton and then incubated in 0.3% H<sub>2</sub>O<sub>2</sub>

in Tris-buffered saline solution for fifteen minutes. A horse-radish peroxidase (HRP)-conjugated goat anti-rabbit secondary antibody (number AP132P; Chemicon Millipore) diluted at a ratio of 1:5000 in Tris-buffered saline solution with 1% bovine serum albumin was applied for one hour at room temperature, then slides were rinsed twice for five minutes in Tris-buffered saline solution and developed with a diaminobenzidine (DAB) chromogen kit (ImmPACT DAB; Vec-

**TABLE I Expression of Cell Surface Markers in Cells Obtained from the Original Tumor and Cells Derived After Mouse Implantation (EACH-1 Cell Line)\***

Marker	Tumor	Cell Line	Marker	Tumor	Cell Line
CD29	98	92	CD36	12	2
CD44	98	96	CD34	11	3
CD49c	94	93	CD11b	11	1
CD59	97	95	CD19	8	3
CD73a	96	96	CD45	8	3
CD105	98	97	CD117	2	5
CD166	98	94	CD3	3	20
CD49b	58	95†	CD184	20	5
CD49f	68	91†	CD79a	13	7
CD90	31	5†	CD106	6	7
CD147	89	27†	CD133	13	4

\*The values are expressed as a percentage of positive cells.

†Reflects a major change in expression.

tor Laboratories, Burlingame, California) for fifteen minutes at room temperature. Slides were counterstained with hematoxylin, dehydrated, cleared, and mounted.

#### Nonadherent Clonogenicity Assay

Single cell suspensions of each cell line were collected, and  $2 \times 10^3$  cells were plated in each well of a six-well Nunc low-cell-binding plate (Nunc, Rochester, New York). Cells were incubated for twelve days before media with colonies was transferred to adherent plates for twenty-four hours, after which colonies were stained with crystal violet. Formation

of colonies with >200 cells was quantified. Clonal density was used as described by Patrawala et al.<sup>12</sup>, and nonadherent plates were used as substitutes for agar plating.

#### Karyotyping

A 150-mm cell culture dish containing a 50% confluent cell population was trypsinized. The pellet was resuspended in a 75-mM KCl solution and was fixed in methanol and acetic acid (in a 3:1 solution). After two washes in fixative, cells were spread on a slide and air-dried, then treated with RNase (0.1 mg/mL) for one hour at 37°C, washed in 2X SSC (saline-sodium citrate buffer), and incubated for five minutes at 37°C in 0.005% pepsin. Slides were then washed in phosphate-buffered saline solution, fixed in 1% formaldehyde, and dehydrated. After the slides were air-dried, they were aged for at least one week at room temperature before denaturation. Some slides were stained in Giemsa (4% in phosphate-buffered saline solution) for scoring dicentric chromosomes. At least 100 Giemsa-stained cells were analyzed for each point, with use of a bright-field microscope.

#### Source of Funding

This research was supported by the Louisiana Cancer Research Consortium; HCA—The Healthcare Company; and the Louisiana Gene Therapy Research Consortium. None of these agencies played a role in the investigation.

#### Results

A growth curve of EACH-1 showed a doubling-time of thirty-seven hours (Fig. 4-A). The cell line was maintained in culture for at least thirty passages, after which it entered into crisis; we noted that brachyury expression decreased with passage (Fig. 4-B).

Compared with the original cells obtained just after the direct tumor culture, we observed in the EACH-1 cell line an

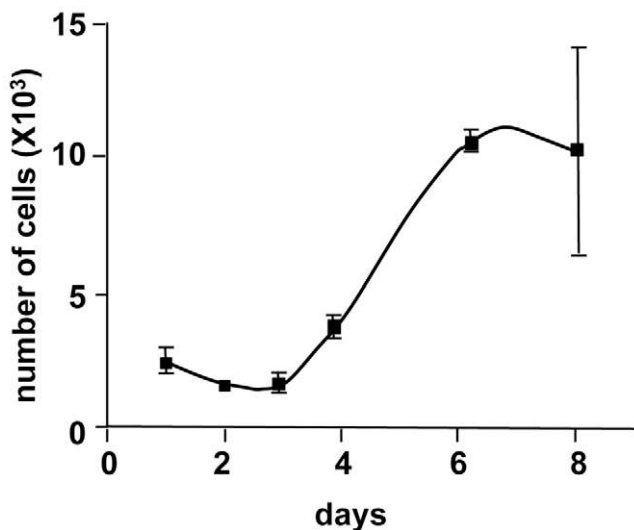


Fig. 4-A

**Fig. 4-A** Growth curve of EACH-1 cell line from three cultures. Error bars indicate the standard deviation. **Fig. 4-B** Western blot analysis of EACH-1 cell line at passage 1, 9, and 29 for brachyury (Bry) protein expression.  $\beta$ -actin is used as internal loading control.

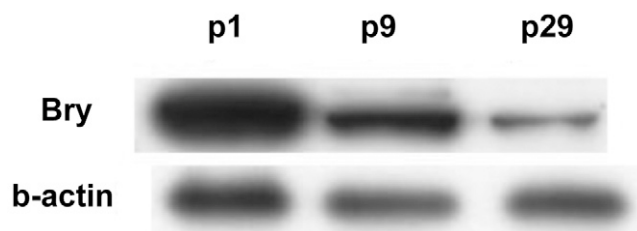


Fig. 4-B

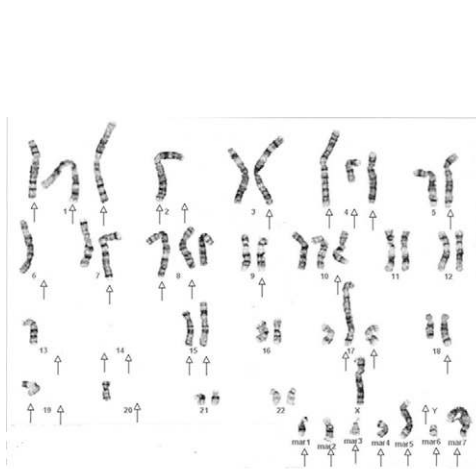


Fig. 5-A

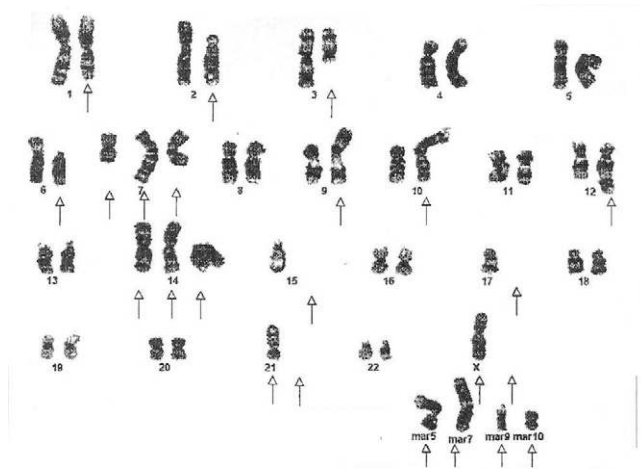


Fig. 5-B

Karyotypes of two distinct clones (Figs. 5-A and 5-B) from the EACH-1 cell line.

increase of positive cells for the cell surface marker CD49f (68% to 91%) and for CD49b (58% to 95%). At the same time, we observed a decrease of CD90 (31% to 5%) and CD147 (89% to 27%). EACH-1 cells are also highly positive (>90%) for CD29, CD44, CD49c, CD59, CD73a, CD105, and CD166 (Table I).

Cytogenetic analysis on twenty-one metaphases by the G bands method with use of trypsin and Wright staining showed unrelated diploid or hypotetraploid clones with aberrations, including loss or gain, of whole or part of multiple chromosomes and chromosome rearrangements. The net imbalances for the first clone are  $-Y, 2p-, +5q, 6p-, +9q, +14q, -5, -17, -21$ , and four to six different marker chromosomes of unknown origin (Fig. 5-A). The net imbalances of the second clone are  $-Y, -1p, -2, +10, -14, -16, +17, +20$ , and four to eight different marker chromosomes of unknown origin (Fig. 5-B). There are also many unknown chromosome materials added to different chromosomes in both clones.

To monitor anchorage-independent growth, we cultured cells under nonadherent conditions. After the cells had been in culture for three weeks, we observed the formation of colonies (Fig. 6-A; right panel), a characteristic of transformed cells. In addition, we tested the clonogenicity of the EACH-1 cell line. The ability to form colonies remained the same if cells were incubated in suspension during six or twelve days. This ability to survive a prolonged time without attachment is also a characteristic of transformed cells (Fig. 6-B). We conducted a serial subcutaneous transplantation of the tumor cell line in *nu/nu* mice that led to tumor formation after three to four weeks (Fig. 6-C). On histological examination, the tumors that developed in the nude mice closely resembled the original patient tumor, and no spread into other mouse organs, including the lungs, was observed.

## Discussion

An extra-axial chordoma has all of the characteristics of a chordoma but is found in the extra-axial skeleton, as the

name implies. Very few have been described<sup>9,13-15</sup>. The criteria for distinguishing an extra-axial chordoma from other similar neoplasms, such as a parachordoma, malignant myoepithelioma, or extra-skeletal myxoid chondrosarcoma, are controversial. Parachordoma is a rare soft-tissue tumor, which is slow growing and usually found adjacent to tendon, synovium, or osseous structures<sup>4,16</sup>. It was once thought to be an extra-axial chordoma, but it was found to have a very different immunohistochemical profile. One difference was a trend for CK-7 to be negative in a parachordoma (as in our patient) and positive in a chordoma<sup>16</sup>. However, Tirabosco et al.<sup>7</sup> described a series of ten extra-axial chordomas, of which only one had a positive CK-7. Extraskeletal myxoid chondrosarcoma was also in the differential; however, it usually has a negative reaction with keratin and epithelial membrane antigen<sup>6,17,18</sup>. Both cytokeratin AE1/AE3 and epithelial membrane antigen were positive in our patient. There is morphological overlap with cartilaginous tumors and chordomas, as there is a relationship between cartilage and the notochord<sup>19</sup>. Currently, the only available technique to characterize a chordoma is immunohistochemical assay for brachyury<sup>7,19,20</sup>. Furthermore, the discovery of brachyury differentially being expressed in chordomas has helped to eliminate the diagnosis of extraskeletal myxoid chondrosarcoma<sup>7,8,19,21</sup>.

Brachyury is a T-box transcription factor, which is essential for the specification of the posterior mesoderm, and regulates notochord formation<sup>17-19</sup>. It is the first protein, to our knowledge, to link axial chordomas histogenetically to the notochord<sup>17-19</sup>. Vujovic et al. suggested that brachyury was only detected by reverse transcription-polymerase chain reaction in chordomas and no other tumor<sup>8</sup>. These findings point to brachyury being a specific marker for chordomas and notochord-derived tumors. We reported the progressive loss of brachyury expression observed along extensive culture of the cell line derived from the tumor (Fig. 3-C). This can be explained by a progressive dedifferentiation of tumor cells that occurs frequently *in vitro*<sup>22</sup>. Further examination of extra-axial chordomas will help us to understand the role of genetic in-



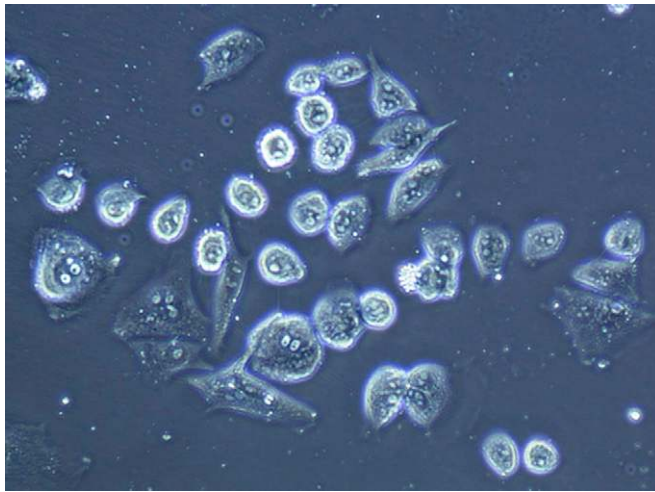


Fig. 6-A

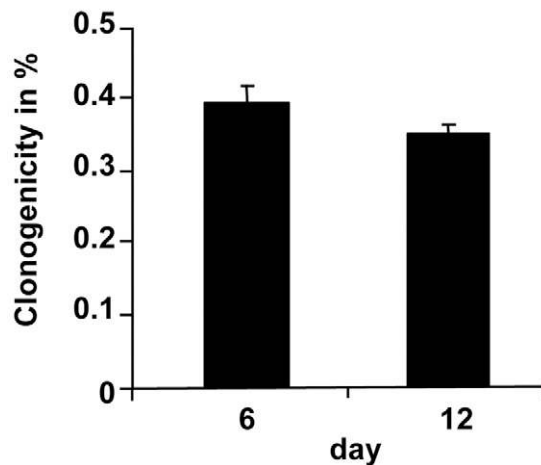
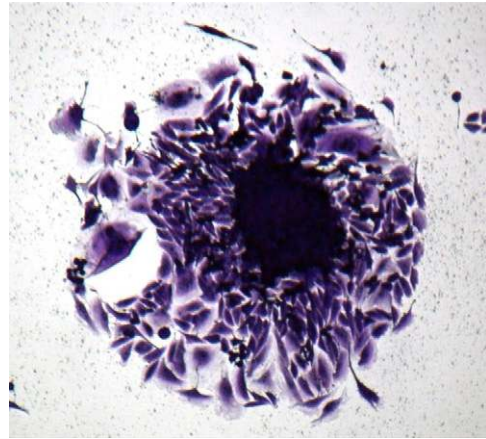


Fig. 6-B

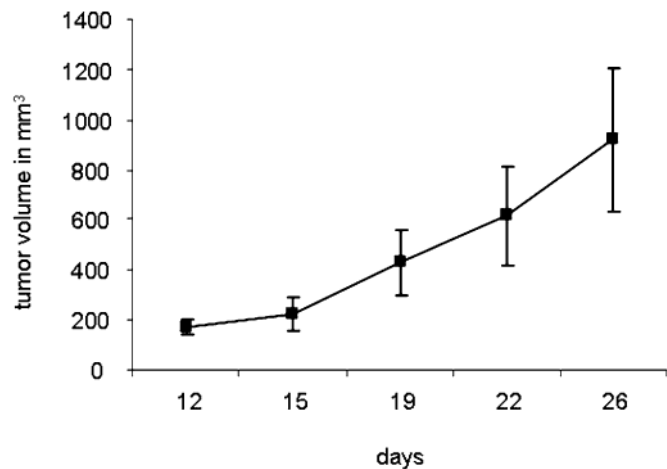


Fig. 6-C

**Fig. 6-A** The left panel shows the morphology of EACH-1 cells ( $\times 200$ ), and the right panel shows formation of a colony from soft agar assay ( $\times 100$ ). **Fig. 6-B** The clonogenicity score after six and twelve days of culture in suspension. The errors bars represent the standard deviation. **Fig. 6-C** Tumor growth curve after subcutaneous injection of ten million EACH-1 cells in three *nu/nu* mice. The error bars represent the standard deviation.

stability in these tumors<sup>23-26</sup>. We believe that the similarities in the histological characteristics of the cultivated tumors, along with the preservation of the brachyury stain (though decreased with ongoing passage), indicate that the cell line is suitable for use in further investigations.

Cytogenetics on EACH-1 cell line clones revealed aberrations that have been previously observed in other chordomas as losses on chromosome arm 1p and 2p or as gains on 5q and 20. These genetic changes associated with chromosome instability are believed to play an important role in tumorigenesis and recurrence of chordomas<sup>27,28</sup>. The establishment of EACH-1, a new chordoma-derived cell line, could represent an interesting tool to further research on the development and treatment of this rare neoplasm. ■

NOTE: The authors thank pathologists Barry F. Faust, MD, of the Ochsner Health System, New Orleans, Louisiana; Jorge E. Ruiz, MD, of the Mayo Medical Laboratories, Jacksonville, Florida;

John Reith, MD, of the University of Florida, Gainesville, Florida; and Adrienne Flanagan, MD, PhD, of University College of London, United Kingdom, for the diagnostics of the tumor; Alan Tucker of the FACS analysis core of the Gene Therapy Center, New Orleans, Louisiana, for the cell surface marker analysis; and Marilyn Li, MD, of the Cytogenetics Core of Tulane Medical School, New Orleans, Louisiana, for the karyotyping.

Amalia M. DeComas, MD  
Department of Orthopaedics,  
University of Texas M.D. Anderson Cancer Center,  
1400 Pressler Boulevard, Suite FCT 10.5067, Houston, TX 77030

Patrice Penfornis, MSc  
Michael R. Harris, BSc  
Radhika R. Pochampally, PhD  
Tulane Center for Gene Therapy,  
Tulane University Health Sciences Center,

JBJS Building, 1324 Tulane Avenue,  
SL-99, New Orleans, LA 70112.  
E-mail address for R.R. Pochampally:  
rpocham@tulane.edu

Mark S. Meyer, MD  
Department of Orthopaedics,  
Ochsner Medical Center,  
1514 Jefferson Highway, New Orleans, LA 70121

## References

- Bjornsson J, Wold LE, Ebersold MJ, Laws ER. Chordoma of the mobile spine. A clinicopathologic analysis of 40 patients. *Cancer*. 1993;71:735-40.
- McMaster ML, Goldstein AM, Bromley CM, Ishibe N, Parry DM. Chordoma: incidence and survival patterns in the United States, 1973-1995. *Cancer Causes Control*. 2001;12:1-11.
- Heffelfinger MJ, Dahlin DC, MacCarty CS, Beabout JW. Chordomas and cartilaginous tumors at the skull base. *Cancer*. 1973;32:410-20.
- Folpe AL, Agoff SN, Willis J, Weiss SW. Parachordoma is immunohistochemically and cytogenetically distinct from axial chordoma and extraskeletal myxoid chondrosarcoma. *Am J Surg Pathol*. 1999;23:1059-67.
- Kilpatrick SE, Hitchcock MG, Kraus MD, Calonje E, Fletcher CD. Mixed tumors and myoepitheliomas of soft tissue: a clinicopathologic study of 19 cases with a unifying concept. *Am J Surg Pathol*. 1997;21:13-22.
- Miettinen M, Lehto VP, Dahl D, Virtanen I. Differential diagnosis of chordoma, chondroid, and ependymal tumors as aided by anti-intermediate filament antibodies. *Am J Pathol*. 1983;112:160-9.
- Tirabosco R, Mangham DC, Rosenberg AE, Vujovic S, Bousdras K, Pizzolitto S, De Maglio G, den Bakker MA, Di Francesco L, Kalil RK, Athanasou NA, O'Donnell P, McCarthy EF, Flanagan AM. Brachyury expression in extra-axial skeletal and soft tissue chordomas: a marker that distinguishes chordoma from mixed tumor/myoepithelioma/parachordoma in soft tissue. *Am J Surg Pathol*. 2008;32:572-80.
- Vujovic S, Henderson S, Presneau N, Odell E, Jacques TS, Tirabosco R, Boshoff C, Flanagan AM. Brachyury, a crucial regulator of notochordal development, is a novel biomarker for chordomas. *J Pathol*. 2006;209:157-65.
- DiFrancesco LM, Davanzo Castillo CA, Temple WJ. Extra-axial chordoma. *Arch Pathol Lab Med*. 2006;130:1871-4.
- Fuchs B, Dickey ID, Yaszemski MJ, Inwards CY, Sim FH. Operative management of sacral chordoma. *J Bone Joint Surg Am*. 2005;87:2211-6.
- Dominici M, Le Blanc K, Mueller I, Slaper-Cortenbach I, Marini F, Krause D, Deans R, Keating A, Prockop DJ, Horwitz E. Minimal criteria for defining multipotent mesenchymal stromal cells. The International Society for Cellular Therapy position statement. *Cytotherapy*. 2006;8:315-7.
- Patrawala L, Calhoun T, Schneider-Broussard R, Li H, Bhatia B, Tang S, Reilly JG, Chandra D, Zhou J, Claypool K, Coghlan L, Tang DG. Highly purified CD44+ prostate cancer cells from xenograft human tumors are enriched in tumorigenic and metastatic progenitor cells. *Oncogene*. 2006;25:1696-708.
- Cesinaro AM, Maiorana A, Collina G, Fano RA. Extra-axial chordoma. Report of a case with immunohistochemical study. *Pathologica*. 1993;85:755-60.
- O'Donnell P, Tirabosco R, Vujovic S, Bartlett W, Briggs TW, Henderson S, Boshoff C, Flanagan AM. Diagnosing an extra-axial chordoma of the proximal tibia with the help of brachyury, a molecule required for notochordal differentiation. *Skeletal Radiol*. 2007;36:59-65.
- Park SY, Kim SR, Choe YH, Lee KY, Park SJ, Lee HB, Jin GY, Jang KY, Lee YC. Extra-axial chordoma presenting as a lung mass. *Respiration*. 2009;77:219-23.
- Fisher C. Parachordoma exists—but what is it? *Adv Anat Pathol*. 2000;7:141-8.
- Bouropoulou V, Kontogeorgos G, Papamichales G, Bosse A, Roessner A, Vollmer E. Differential diagnosis of chordoma immunohistochemical aspects. *Arch Anat Cytol Pathol*. 1987;35:35-40.
- Wiebe BM, Jensen K, Laursen H. Parachordoma of the sacrococcygeal region—a neuroepithelial tumor. *Clin Neuropathol*. 1995;14:343-6.
- Romeo S, Hogendoorn PC. Brachyury and chordoma: the chondroid-chordoid dilemma resolved? *J Pathol*. 2006;209:143-6.
- Kilpatrick SE, Limon J. Mixed tumour/ myoepithelioma/ parachordoma. In: Fletcher CDM, Unni KK, Mertens F, editors. *World Health Organization Classification of Tumours. Pathology and Genetics. Tumours of Soft Tissue and Bone*. Lyon, France: IARC Press; 2002. p 198-9.
- Oakley GJ, Fuhrer K, Seethala RR. Brachyury, SOX-9, and podoplanin, new markers in the skull base chordoma vs chondrosarcoma differential: a tissue microarray-based comparative analysis. *Mod Pathol*. 2008;21:1461-9.
- Diamandopoulos GT, Miller MH, McLane MF, Evans PG. Loss or persistence of the differentiated state of simian virus 40-induced hamster tumor cells before and after serial passage in culture. *Cancer Res*. 1976;36(9 pt 1):3171-7.
- Heim S, Mitelman F. *Cancer cytogenetics*. New York: Wiley Blackwell; 2009. p 1-31.
- Anderson GR, Stoler DL, Brenner BM. Cancer: the evolved consequence of a destabilized genome. *Bioessays*. 2001;23:1037-46.
- Lengauer C, Kinzler KW, Vogelstein B. Genetic instabilities in human cancers. *Nature*. 1998;396:643-9.
- Loeb LA. A mutator phenotype in cancer. *Cancer Res*. 2001;61:3230-9.
- Scheil S, Bruderlein S, Liehr T, Starke H, Herms J, Schulte M, Möller P. Genome-wide analysis of sixteen chordomas by comparative genomic hybridization and cytogenetics of the first human chordoma cell line, U-CH1. *Genes Chromosomes Cancer*. 2001;32:203-11.
- Larson BL, Ylöstalo J, Prockop DJ. Human multipotent stromal cells undergo sharp transition from division to development in culture. *Stem Cells*. 2008;26:193-201.